Biomacromolecules

pubs.acs.org/Biomac

Article

2,5-Anhydro-D-Mannose End-Functionalized Chitin Oligomers Activated by Dioxyamines or Dihydrazides as Precursors of Diblock Oligosaccharides

Ingrid Vikøren Mo, Marianne Øksnes Dalheim, Finn L. Aachmann, Christophe Schatz,* and Bjørn E. Christensen*

Cite This: *Biomacromolecules* 2020, 21, 2884–2895

Read Online

ACCESS | Metrics & More | Article Recommendations | Supporting Information

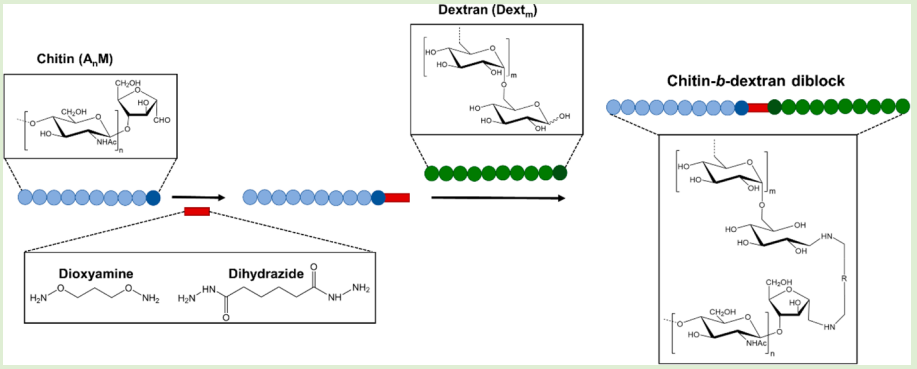

ABSTRACT: Diblock oligosaccharides based on renewable resources allow for a range of new but, so far, little explored biomaterials. Coupling of blocks through their reducing ends ensures retention of many of their intrinsic properties that otherwise are perturbed in classical lateral modifications. Chitin is an abundant, biodegradable, bioactive, and self-assembling polysaccharide. However, most coupling protocols relevant for chitin blocks have shortcomings. Here we exploit the highly reactive 2,5-anhydro-D-mannose residue at the reducing end of chitin oligomers obtained by nitrous acid depolymerization. Subsequent activation by dihydrazides or dioxyamines provides precursors for chitin-based diblock oligosaccharides. These reactions are much faster than for other carbohydrates, and only acyclic imines (hydrazones or oximes) are formed (no cyclic *N*-glycosides). α-Picoline borane and cyanoborohydride are effective reductants of imines, but in contrast to most other carbohydrates, they are not selective for the imines in the present case. This could be circumvented by a simple two-step procedure. Attachment of a second block to hydrazide- or aminooxy-functionalized chitin oligomers turned out to be even faster than the attachment of the first block. The study provides simple protocols for the preparation of chitin-*b*-chitin and chitin-*b*-dextran diblock oligosaccharides without involving protection/deprotection strategies.

INTRODUCTION

Block polysaccharides are a new class of engineered polymers based on renewable resources.[1,2] Among these, diblock polysaccharides, which are composed of two different oligo- or polysaccharide blocks (Figure 1), represent the simplest type. By attaching the blocks at the chain termini, their intrinsic properties are minimally perturbed.[3,4] In this respect, they are analogous to synthetic AB-type block copolymers. However, the broad range of chemical, physical, and biological properties of natural and abundant polysaccharides is very different from most synthetic blocks. Examples include solubility, crystallinity, interactions with ions, pH responses, and above all, biodegradability. This work focuses on the preparation of chitin-based diblock oligosaccharides by using the dihydrazide/dioxyamine copper-free and aniline-free conjugation methodology recently applied to chitosan oligosaccharides having a *N*-acetyl-D-glucosamine (GlcNAc) residue at the reducing end.[5] Here we take advantage of chitins with a reactive 2,5-anhydro-D-mannose residue at the reducing end. In contrast to alkyne/azide click chemistry, where each block needs to be modified prior to coupling,[6−9] our methodology takes advantage of the native reducing end for attachment of blocks to bivalent dihydrazides and dioxyamines (Figure 1).

Received: April 23, 2020
Revised: June 11, 2020
Published: June 15, 2020

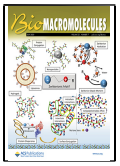

https://dx.doi.org/10.1021/acs.biomac.0c00620
Biomacromolecules 2020, 21, 2884–2895

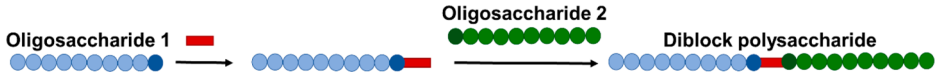

Figure 1. Preparation of a diblock polysaccharide by a two-step strategy. First, a bivalent linker is attached to the reducing end of oligosaccharide 1. Oligosaccharide 2 is subsequently attached.

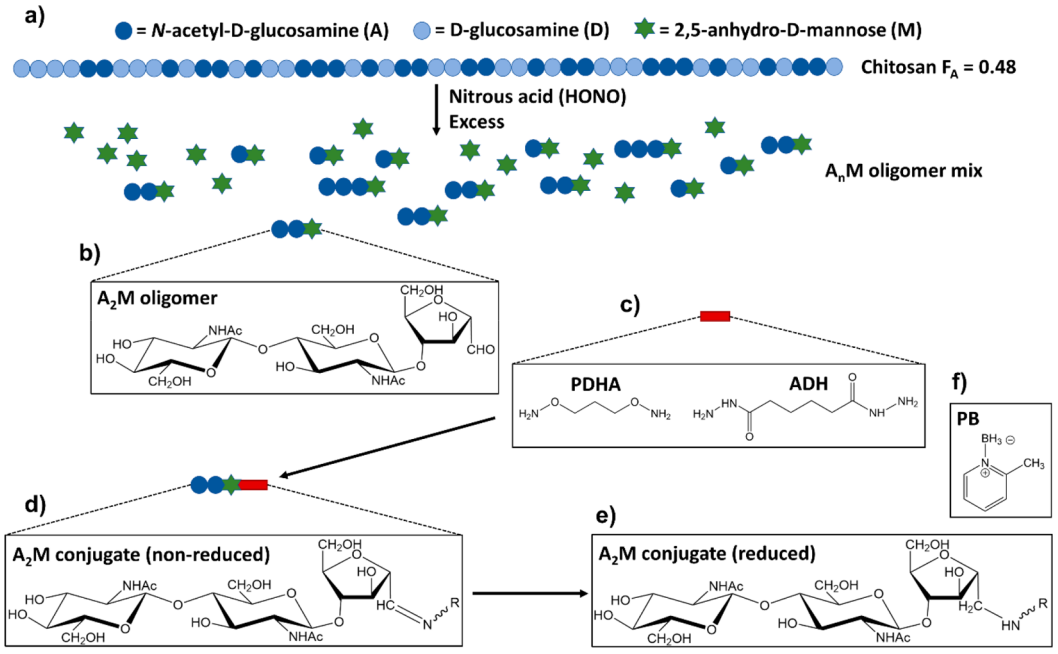

Figure 2. (a) Preparation of chitin oligomers (A_nM) by degradation of chitosan (e.g., F_A = 0.48) using an excess nitrous acid (HONO). (b) Chemical structure of an A_2M oligomer. (c) Chemical structure of PDHA and ADH. (d) Chemical structure of a nonreduced A_2M conjugate. (e) Chemical structure of a reduced A_2M conjugate. (f) Chemical structure of PB.

Chitin is a component of the exoskeleton of shrimp and crabs and is available in large quantities as a byproduct in aquaculture. It is exclusively composed of β-1,4-linked GlcNAc (A) residues and, consequently, the fraction of acetylated units (F_A) is 1. Chitin has self-assembly properties and becomes water insoluble and crystalline above DP 6. In contrast to chitosans, which can be obtained by partial de-*N*-acetylation of chitin (F_A < 1), it is not responsive to changes in pH. Chitin can be degraded by chitinases or by chemical methods to form chitooligosaccharides, which may have biological effects, including eliciting defense responses in plants and anticancer properties in animals.[10−13] Enzymatically degradable chitin−cellulose[14] and chitin−poly(propylene glycol)[15] diblocks have been described in the literature. However, their synthesis involved protection/deprotection of hydroxyls and diisocyanate coupling via the natural reducing ends.

Nitrous acid (HONO) depolymerization of chitosan (Figure 2a) is a commonly used alternative to enzymatic degradation or acid hydrolysis to prepare chitooligosaccharides with a 2,5-anhydro-D-mannose (M) residue at the reducing end.[16,17] The HONO only affects the D-glucosamine (GlcN, D) residues of the chitosan and, hence, chitin oligomers (A_nM) can be obtained by using an excess HONO to the fraction of D residues ($F_D = 1 - F_A$). The pending aldehyde of the M residue (Figure 2b) makes such oligomers particularly reactive. This has been exploited to prepare self-branched chitosans[18] as well as a range of end-activated chitosan oligomers for subsequent preparation of chitosan-based copolymers.[3,19−21] In contrast, block polysaccharides exploiting A_nM chitin oligomers have to our knowledge not been explored.

Here we report the conjugation of chitin oligomers of the type A_nM (where *n* refers to the number of A residues; hence, the degree of polymerization (DP) = *n* + 1) to adipic acid dihydrazide (ADH) and *O*,*O*′-1,3-propanediyl-bishydroxylamine (PDHA) as the first step to form activated chitin oligomers (A_nM-ADH and A_nM-PDHA; Figure 2b−d). The study includes the irreversible reduction of conjugates to form stable secondary amine conjugates (Figure 2e) using α-picoline borane (PB) as reductant (Figure 2f).[5,22−25] In the second step, we explore, in a similar way, the attachment of a second oligosaccharide block to both ADH- and PDHA-activated A_nM to prepare two different chitin-based diblocks with antiparallel chains: A_nM-*b*-MA_n and A_nM-*b*-$Dext_m$. $Dext_m$ refers to dextran oligomers with *m* residues. Dextran is a neutral and flexible polysaccharide composed of D-glucose residues linked by α-1,6-linkages, with some short branches.[26,27] The diblocks were purified by gel filtration chromatography (GFC) and characterized by NMR. The outcome of the study includes kinetic and structural data for each conjugation step as well as protocols for preparing activated oligosaccharides and pure diblock polysaccharides, the latter forming a basis for future structure−function studies.

MATERIALS AND METHODS

Materials. High molecular weight chitosan (F_A = 0.48, [η] = 1210 mL/g) was obtained from Advanced Biopolymers (Norway). The fraction of acetylated units (F_A) was confirmed by ^{1}H NMR spectroscopy.[28] Dextran T-2000 (M_w = 2000000 g/mol) was obtained from Pharmacia Fine Chemicals. Adipic acid dihydrazide (ADH), *O*,*O*′-1,3-propanediylbishydroxylamine dihydrochloride (PDHA), and 2-methylpyridine borane complex (α-picoline borane, PB) were

https://dx.doi.org/10.1021/acs.biomac.0c00620
Biomacromolecules 2020, 21, 2884−2895

obtained from Sigma-Aldrich. All other chemicals were obtained from commercial sources and were of analytical grade.

Gel Filtration Chromatography (GFC). Preparative and analytical gel filtration chromatography (GFC) were used for fractionation of chitin oligosaccharides and fractionation of products, respectively, as described earlier.[5] In brief, both systems were composed of Superdex 30 columns (BPG 140/950 (140 mm × 95 cm) and HiLoad 26/600 (26 mm × 60 cm), respectively) connected in series, continuously eluting ammonium acetate (AmAc) buffer (0.15 M, pH 4.5 and 0.1 M, pH 6.9, respectively). Fractionation was monitored online using a refractive index (RI) detector and fractions were collected and pooled according to elution times. The pooled fractions were reduced to appropriate volumes, dialyzed (MWCO = 100−500 Da) against ultrapure Milli-Q (MQ) water until the measured conductivity of the water was <2 μS/cm and freeze-dried or freeze-dried directly without dialysis.

NMR Spectroscopy. Samples for NMR characterization were dissolved in D_2O (450−600 μL, approx. 10 mg/mL). For some samples, 1% sodium 3-(trimethylsilyl)-propionate-d_4 (TSP, 3 μL) was added as an internal standard. Samples for the time course NMR experiments were prepared in deuterated NaAc buffer (500 mM, pH = 3.0, 4.0, or 5.0, 2 mM TSP).

All homo- and heteronuclear NMR experiments were carried out on a Bruker Ascend 14.1 T 600 MHz or a Bruker Ascend 18.8 T 800 MHz spectrometer (Bruker BioSpin AG, Fällanden, Switzerland), both equipped with Avance III HD electronics and a 5 mm Z-gradient CP-TCI cryogenic probe.

Characterization of oligomers, purified conjugates or other products was performed by obtaining 1D ^{1}H NMR spectra at 300 K on the 600 MHz spectrometer. Time-course experiments were performed by obtaining 1D ^{1}H NMR spectra at specific time points at 300 K on the 600 MHz spectrometer. Chemical shift assignments were performed at 298 K on the 800 MHz spectrometer by obtaining the following homo- and heteronuclear NMR spectra: 1D proton, 2D double quantum filtered correlation spectroscopy (DQF-COSY), 2D total correlation spectroscopy (TOCSY) with 70 ms mixing time, 2D ^{13}C heteronuclear single quantum coherence (HSQC) with multiplicity editing, 2D ^{13}C heteronuclear 2 bond correlation (H2BC), 2D ^{13}C HSQC-[^{1}H,^{1}H]TOCSY with 70 ms mixing time on protons, and 2D heteronuclear multiple bond correlation (HMBC) with BIRD filter to suppress first order correlations.

All spectra were recorded, processed, and analyzed using TopSpin 3.5pl7 software (Bruker BioSpin).

Preparation of Chitin Oligomers by Nitrous Acid Degradation. Chitosan (F_A = 0.48, 20 mg/mL) was dissolved in acetic acid (AcOH, 2.5 vol %) by stirring overnight. Dissolved oxygen was removed by bubbling the solution with N_2 gas for 15 min. After cooling the solution to approximately 4 °C, a freshly prepared $NaNO_2$ solution (20 mg/mL, 30% excess mole $NaNO_2$: mole D-units) was added in three portions with 45 min intervals. The reaction mixture was agitated in the dark at 4 °C overnight on a shaking device to ensure complete degradation. The degradation mixture was centrifuged using an Allegra X-15R centrifuge (Beckman Coulter) equipped with a SX4750A rotor (30 min, 4750 rpm), and the pellet was washed with AcOH (2.5 vol %). The washing and centrifugation steps were repeated three times to remove insoluble high molecular weight chitin oligomers. The supernatant (containing water-soluble low molecular weight chitin oligomers) was filtered (5 and 45 μm) and freeze-dried. The water-soluble chitin oligomers (DP < 10) were fractionated according to a degree of polymerization (DP) using the preparative GFC system (0.15 M AmAc, pH 4.5). Oligomer fractions were dialyzed (MWCO = 100−500) against MQ-water until the measured conductivity was <2 μS/cm and freeze-dried. Purified oligomers were characterized by 1D ^{1}H NMR (600 MHz spectrometer).

Preparation of Dextran Oligomers by Acid Degradation. Dextran T-2000 (M_w = 2000000, 50 mg/mL) was dissolved in MQ-water overnight. HCl (0.1 M) was added to give a final concentration of 0.05 M HCl and 25 mg/mL dextran. Degradation was performed at 95 °C for 12 h. The degradation mixture was fractionated using the preparative GFC system to obtain dextran oligomers ($Dext_m$) of specific DP (m = DP). $Dext_m$ oligomers were purified by dialysis as above and characterized by 1D ^{1}H NMR (600 MHz spectrometer).

Conjugation and Reduction Studied by Time-Course NMR. Time-course NMR experiments were performed as described earlier.[5] In brief, chitin oligomers (A_nM) or dextran oligomers ($Dext_m$; 20.1 mM) and 2 equiv ADH or PDHA (40.2 mM) were dissolved separately in deuterated NaAc buffer (500 mM, pH = 3.0, 4.0 or 5.0, 2 mM TSP) and transferred to a 5 mm NMR tube. For the time-course reduction experiments, 3 equiv (60.3 mM) of PB or 3 or 10 equiv (60.3 or 201 mM) of $NaCNBH_3$ were added directly to the NMR tube with equilibrium mixtures of conjugates. Concentrations given in parentheses are final concentrations after mixing. Mixing of reagents in the NMR tube or addition of reducing agent served as time zero (t = 0). 1D ^{1}H NMR spectra were recorded at desired time points (600 MHz spectrometer, 300 K), and the course of the reactions was tracked by integration of the spectra. Samples were held at room temperature between recordings. Equilibrium yields and yields from the reduction of conjugates in the NMR tube were obtained by integration of the ^{1}H NMR spectra.

For experiments where a large excess of PB (20 equiv) was used, equilibrium mixtures with nonreduced conjugates were removed from the NMR tube and reduced in a separate vial.

Preparative Protocol for Reduced Conjugates (Activated Chitin Oligomers). Chitin oligomers (A_nM, 20.1 mM) and 10 equiv of ADH or PDHA (201 mM) were dissolved in NaAc buffer (500 mM, pH 4.0) to which 3 or 20 equiv of PB (60.3 or 420 mM), respectively, were added after >6 h. The reduction was performed at room temperature for 24 or 48 h for A_nM-ADH or A_nM-PDHA conjugates, respectively. Reactions were terminated by dialysis (MWCO = 100−500 Da) against 0.05 M NaCl until the insoluble PB was dissolved and, subsequently, freeze-dried. Conjugates were purified by GFC (analytical scale) and freeze-dried directly several times to remove the volatile GFC buffer (0.1 M AmAc). Purified conjugates were characterized by NMR spectroscopy (600 MHz spectrometer). Chemical shift assignment for the purified A_2M-PDHA conjugate was performed by homo- and heteronuclear NMR spectroscopy (800 MHz spectrometer).

Preparation of Chitin Diblock Structures Using a Substoichiometric Amount of ADH or PDHA. Chitin oligomers (A_nM, 20.1 mM) and 0.5 equiv of PDHA or ADH (10.05 mM) were dissolved in deuterated NaAc buffer (500 mM, pH 4.0) and the conjugation was studied by time-course NMR, as described above. Reduction with 3 or 20 equiv PB, fractionation, and characterization of products were performed as described for the preparative protocol, however, with a longer reduction time (96 h) for the diblocks formed with PDHA.

Preparation of Diblock Structures from Activated Chitin Oligomers. Purified chitin oligomer conjugates (A_nM-ADH or A_nM-PDHA, 20.1 mM) were reacted with equimolar concentrations of chitin oligomers (A_nM) or dextran oligomers ($Dext_m$) to form diblock structures (in 500 mM deuterated NaAc buffer, pH 4.0, RT). The conjugation of the second block was monitored by time-course ^{1}H NMR until equilibrium was reached. Reduction of chitin diblocks (A_nM-b-MA_n) was performed as described for the preparative protocol using 3 equiv PB. Due to slow reduction of $Dext_m$ conjugates, reduction was performed using 20 equiv (402 mM) PB at 40 °C for 96 h for the A_nM-PDHA-$Dext_m$ diblocks and 144 h for the A_nM-ADH-$Dext_m$ diblocks. Fractionation and characterization of products were performed as above. The relative yield of diblocks was obtained by integration of the GFC chromatogram.

RESULTS AND DISCUSSION

Preparation and Characterization of Chitin Oligomers. Chitin oligomers of the type A_nM were obtained by degrading chitosan using an excess of nitrous acid (HONO) to the fraction of D residues. The mixture of water-soluble chitin oligomers was fractionated by GFC (Supporting Information, S1). Purified oligomers were characterized by

https://dx.doi.org/10.1021/acs.biomac.0c00620
Biomacromolecules 2020, 21, 2884−2895

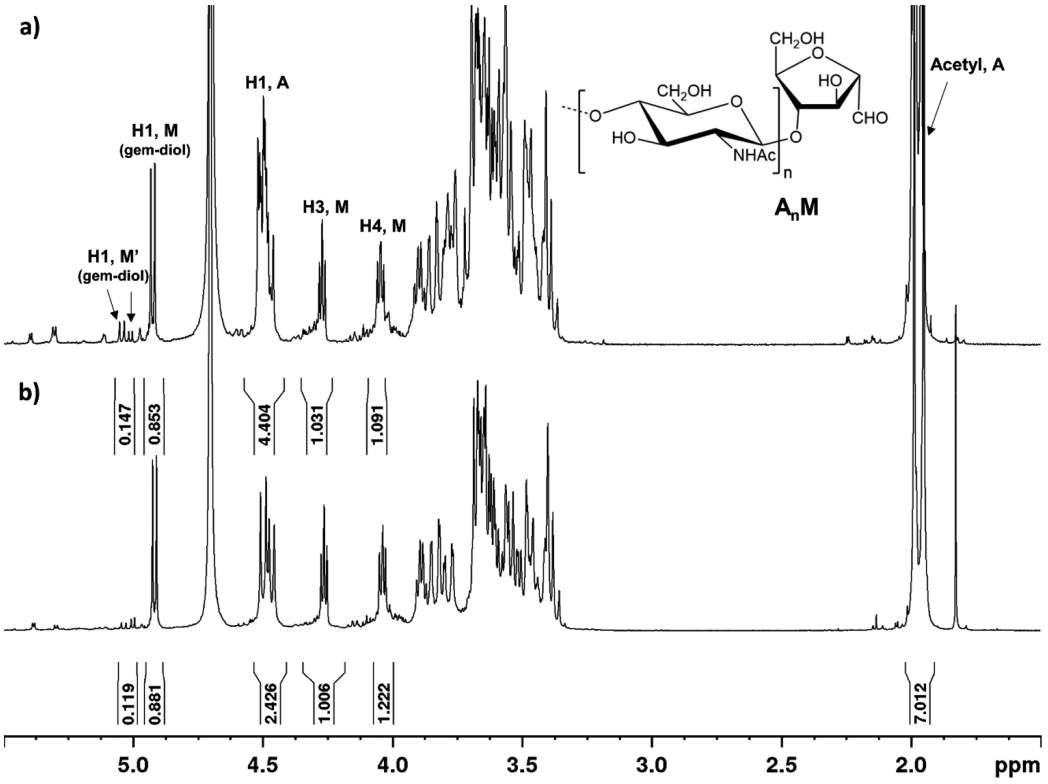

Figure 3. ^{1}H NMR characterization of purified (a) A_4M and (b) A_2M oligomers in D_2O (600 MHz).

^{1}H NMR (Figure 3), and key resonances were annotated according to literature.[17] The reducing end "aldehyde" proton appears as a doublet at 4.9 ppm due to complete hydration in water to the corresponding gem-diol.[17] The minor resonances around 5 ppm (marked as M′ in Figure 3) were tentatively assigned to alternative forms of the M residue predicted in the literature.[29] These alternative forms (<15%) are not easily detected and, in particular, not quantified for longer oligomers of the D_nM type (where n is the number of contiguous uninterrupted D residues)[19] due to weak reducing end resonances. Also, a major difference between A_nM and D_nM oligomers is the requirement for excess HONO in the preparation of the former, which may possibly influence the formation of these alternative M forms.

Reaction with ADH and PDHA. The conjugation of the trisaccharide A_2M to ADH or PDHA (2 equiv) was studied in detail by time course NMR at pH 3.0, 4.0, and 5.0 (Supporting Information, S2). ^{1}H NMR spectra of the equilibrium mixtures for the conjugation reactions at pH 4.0 are given in Figure 4. In agreement with the literature,[19] only *E*-/*Z*-hydrazones or oximes were formed. Minor resonances close to the main resonances for the *E*- and *Z*-hydrazones or oximes were attributed to the conjugation of oligomers with alternative forms of the M residue (marked as H1, M′ in Figure 4).

Kinetics. Kinetic plots for the conjugation of A_2M to ADH (hydrazone formation) and PDHA (oxime formation) are given in Figure 5a and b, respectively. The combined yield is the sum of *E*- and *Z*-hydrazones/oximes for all the forms of the M residue. Compared to chitosan oligomers with GlcNAc (A) at the reducing end,[5] A_nM oligomers reacted much faster with both ADH and PDHA under otherwise identical conditions (results obtained for AA[5] are included in Figure 5). With 2 equiv of ADH or PDHA, reactions were essentially complete after 4−6 h.

Reaction modeling is a powerful tool to simulate reactions, and to predict the effects of, for example, changing the concentration of reactants. We have previously shown that the conjugation of chitosan oligomers (with A at the reducing end) to ADH and PDHA, was first order with respect to each reactant in the range 2−10 equiv.[5] In contrast to these oligomers, the model for A_nM becomes simpler because cyclic *N*-glycosides are not formed. The model is detailed in Supporting Information, S3. The outcome of the modeling is estimated rate constants for the formation and dissociation of *E*-/*Z*-hydrazones and oximes. Rate constants for best fits are given in Table 1. We also included the times to reach 50% and 90% of the combined equilibrium yields ($t_{0.5}$ and $t_{0.9}$; Table 1). This provides a clearer picture when comparing different reactions and reaction protocols and also follows the method devised for other conjugation reactions.[5,30] In general, all experimental data gave relatively good fits, except a slight deviation in the range between 85 and 100% conversion, which can tentatively be attributed to the minor population of alternative forms of the M residue reacting somewhat more slowly (Supporting Information, S4). It may also be noted that the rate constants for the dissociation of *E*- and *Z*-conjugates needed to have the same value in order to obtain the good fits for the data to the model. The kinetics, equilibrium constants, and reaction yield depended slightly on pH, with pH 5.0 giving the fastest reactions in both cases (Table 1). However, pH 4.0 was used in further conjugations due to the pH dependence for the reduction step (see below).

The table includes kinetic data for a higher DP, in this case, the hexamer A_5M. As for the chitosan oligomers studied previously,[5] the reaction kinetics appeared to be essentially independent of DP in the range studied. It may be noted that A_nM becomes gradually less soluble in the buffer when n > 5.

https://dx.doi.org/10.1021/acs.biomac.0c00620
Biomacromolecules 2020, 21, 2884−2895

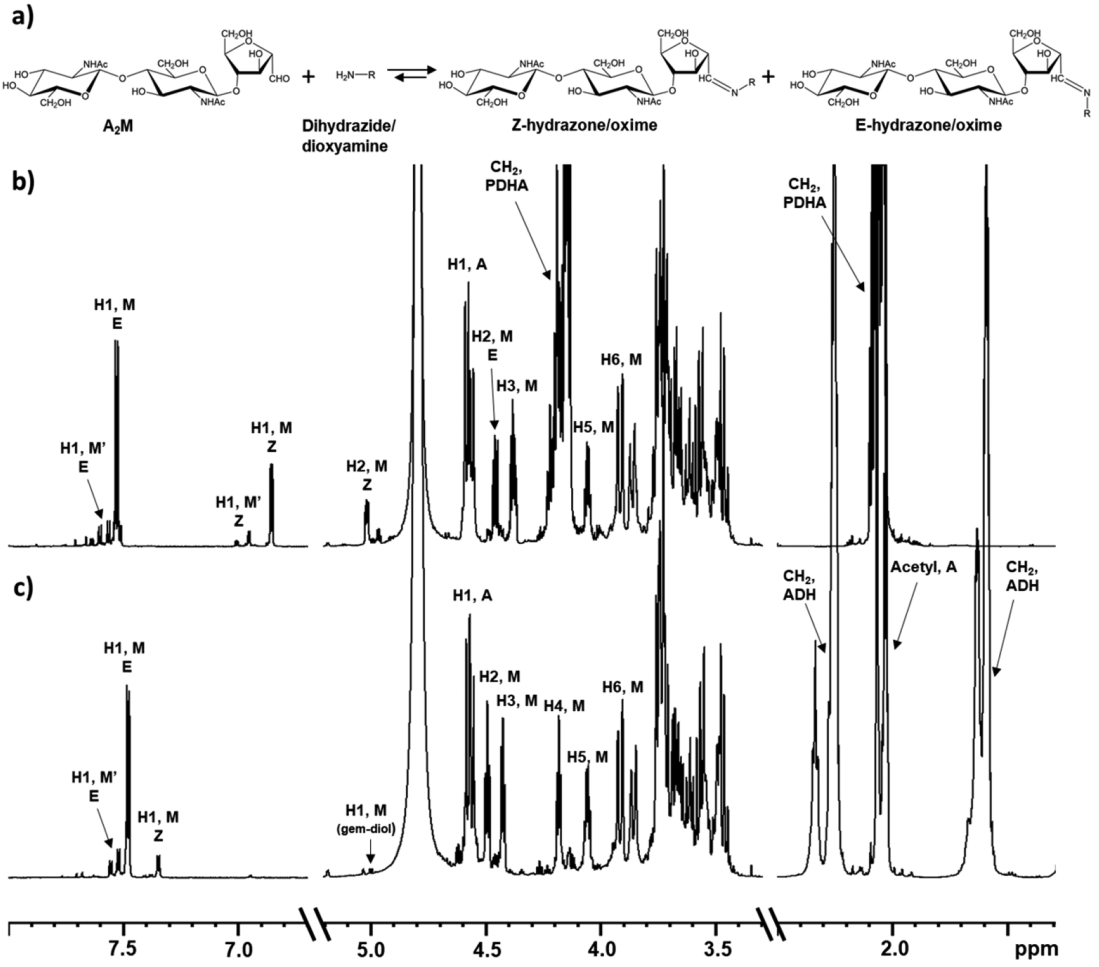

Figure 4. (a) General reaction scheme for the conjugation of A_2M to ADH (dihydrazide) or PDHA (dioxyamine). (b and c) ^1H NMR spectra of the equilibrium mixtures obtained for the conjugation of A_2M to PDHA and ADH, respectively.

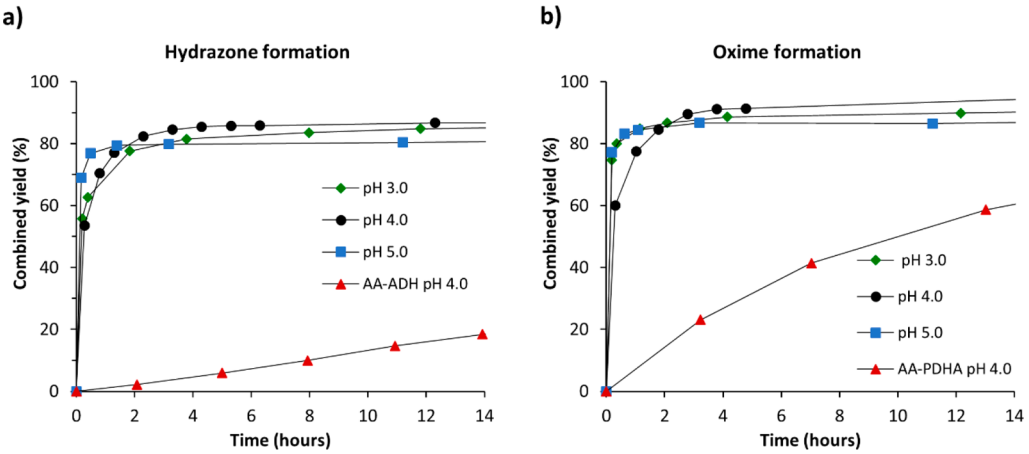

Figure 5. Reaction kinetics for the conjugation of A_2M oligomers (20.1 mM) to 2 equiv of (a) ADH (hydrazone formation) and (b) PDHA (oxime formation) at pH 3.0, 4.0, and 5.0. Kinetics for the conjugation of AA at pH 4.0[5] is included for comparison.

Hence, longer oligomers can therefore not be easily prepared and studied by the present method.

Reduction. Most conjugations of this type are combined with an irreversible reduction step to obtain stable secondary amine conjugates. It was recently confirmed that PB can be a good alternative to sodium cyanoborohydride ($NaCNBH_3$) for similar conjugations of chitosan oligomers with natural reducing ends,[5] prompting us to attempt a similar approach here. Besides being less toxic, PB also spontaneously decomposes more slowly (about 20×) than $NaCNBH_3$ under the given conditions (Supporting Information, S5). Although PB has low solubility in the aqueous buffer at room temperature, stirring was shown to increase the reduction rate, suggesting the reduction also takes place at the surface of the undissolved particles.[5,31]

https://dx.doi.org/10.1021/acs.biomac.0c00620
Biomacromolecules 2020, 21, 2884−2895

Table 1. Kinetic Parameters Obtained from the Modeling of the Conjugation of A (A_nM) to B (ADH, PDHA or A_4M-ADH) Using Different Equivalents of B[a]

		equivalents		A + B ↔ E		A + B ↔ Z				
A	B	B	pH	k_1 (h^{-1})	k_{-1} (h^{-1})	k_2 (h^{-1})	k_{-2} (h^{-1})	$t_{0.5}$ (h)	$t_{0.9}$ (h)	equilibrium yield (%)
A_2M	ADH	2	3.0	3.1×10^{-2}	4.0×10^{-1}	4.1×10^{-3}	4.0×10^{-1}	0.22	0.78	85
A_2M	ADH	2	4.0	1.8×10^{-2}	2.0×10^{-1}	2.5×10^{-3}	2.0×10^{-1}	0.38	1.37	87
A_2M	ADH	2	5.0	4.1×10^{-2}	7.0×10^{-1}	5.8×10^{-3}	7.0×10^{-1}	0.16	0.55	81
A_2M	PDHA	2	3.0	2.8×10^{-2}	2.5×10^{-1}	1.2×10^{-2}	2.5×10^{-1}	0.21	0.75	91
A_2M	PDHA	2	4.0	2.4×10^{-2}	2.2×10^{-1}	1.0×10^{-2}	2.2×10^{-1}	0.24	0.87	91
A_2M	PDHA	2	5.0	3.5×10^{-2}	4.5×10^{-1}	1.6×10^{-2}	4.5×10^{-1}	0.16	0.56	88
A_5M	ADH	2	4.0	3.0×10^{-2}	3.5×10^{-1}	4.0×10^{-3}	3.5×10^{-1}	0.23	0.82	86
A_5M	PDHA	2	4.0	2.3×10^{-2}	8.0×10^{-2}	1.0×10^{-3}	8.0×10^{-2}	0.27	0.97	96
A_2M	ADH	0.5	4.0	4.0×10^{-1}	9.0×10^{-1}	5.8×10^{-2}	9.0×10^{-1}	0.06	0.28	73
A_2M	PDHA	0.5	4.0	1.2×10^{-1}	6.0×10^{-2}	5.2×10^{-2}	6.0×10^{-2}	0.22	1.21	88
A_4M	A_4M-ADH	1	4.0	7.3×10^{-2}	1.5×10^{-1}	1.1×10^{-2}	1.5×10^{-1}	0.35	1.57	74

[a]E: *E*-hydrazone/oxime. Z: *Z*-hydrazone/oxime. Two different models were applied. The first model estimates the individual rate constants for the formation and dissociation of E (k_1 and k_{-1}) and Z (k_2 and k_{-2}), whereas the second model considers the total (E + Z) as a single reaction product, providing times needed to reach 50% and 90% ($t_{0.5}$ and $t_{0.9}$) of the equilibrium yield.

The high reactivity of the pending aldehyde (*gem*-diol) of the M residue, prompted us to first investigate possible reduction of A_nM oligomers, which would render the oligomers unreactive for further conjugation. The reduction by PB was therefore assayed by time course NMR in the pH range 3.0–5.0. Reduction by $NaCNBH_3$ at pH 4.0 was included for comparison. Kinetic data are shown in Figure 6.

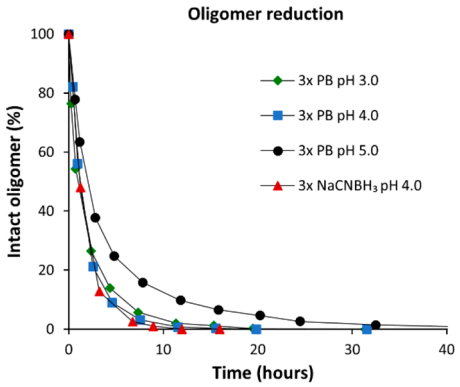

Figure 6. Reaction kinetics for the reduction of A_nM oligomers at pH 3.0, 4.0, and 5.0 using 3 equiv (3×) PB at RT. Reduction at pH 4.0 using 3 equiv $NaCNBH_3$ at RT, is included in the figure for comparison. NMR spectra are shown in Supporting Information, S6.

NMR spectra are given in the Supporting Information, S6. Complete reduction by PB was obtained after approximately 20, 12, and 40 h for pH 3.0, 4.0, and 5.0, respectively. Data were further fitted to a kinetic model assuming the rate of reduction (assumed irreversible) is proportional to the concentrations of each reactant. The rate constants are given in Table 2. With $NaCNBH_3$ reduction was complete after less than 12 h at pH 4.0. These results contrast with those of natural reducing ends such as the AA disaccharide, where no detectable reduction was observed under the same conditions (Supporting Information, S6). Hence, both reductants result in significant reduction of the A_nM oligomers, which directly influences the protocols for reductive amination, as discussed below.

The reduction of A_nM conjugates (oximes and hydrazones) was subsequently investigated by adding PB (3 equiv) to the

Table 2. Rate Constants Obtained for the Reduction of Hydrazones and Oximes by PB (3×) Assuming Both Isomers (*E*-/*Z*-forms) of the Conjugates Are Reduced with the Same Rate[a]

	rate constants (h^{-1})		
pH	3.0	4.0	5.0
A_nM (unreacted oligomer)	1.1×10^{-2}	1.5×10^{-2}	7.0×10^{-3}
A_nM-ADH (hydrazone)	4.0×10^{-2}	1.5×10^{-2}	3.0×10^{-3}
A_nM-PDHA (oxime)	1.5×10^{-3}	4.2×10^{-4}	8.0×10^{-5}[b]

[a]Rate constants for the reduction of oligomers by PB are included for comparison. [b]Inaccurate (initially fast, then slow).

corresponding reaction mixtures after equilibrium was reached (i.e., after >12 h). Bases for the time course NMR analyses were the reduced intensity of the *E*- and *Z*-resonances, as well as emergence of methylene proton resonances of the secondary amine in the ^1H NMR spectra (Supporting Information, S7). Kinetic plots are given in Figure 7.

Hydrazone (A_nM-ADH) reduction with PB (Figure 7a) is indeed very fast in this system, and clearly fastest at pH 3.0, where complete reduction of conjugates is obtained after about 10 h at RT. The reduction here is slightly slower at pH 4.0, and much slower at pH 5.0. The same pH dependence is also observed for oxime (A_nM-PDHA) reduction (Figure 7b), except that the reduction is generally much slower, being complete after about 150–200 h. The pH-dependence of hydrazone and oxime reduction by PB has to our knowledge not been studied in detail, but we attribute the faster reduction at lower pH to the formation of reducible iminium ions by protonation. Hydrazone and oxime reduction by $NaCNBH_3$ (pH 4.0) was also investigated. Complete hydrazone reduction was obtained after approximately 1 h with 3 equiv of $NaCNBH_3$ (Figure 7a). Oxime reduction was slower under the same conditions, however, with an initial rate similar to that of PB at pH 3.0 (Figure 7b). Due to the rapid decomposition of $NaCNBH_3$ in the buffer, 3 equiv were insufficient to reach completion, leveling off at approximately 90% yield. In contrast to PB, which is poorly soluble at higher concentrations, 10 equiv of $NaCNBH_3$ could be completely dissolved, enabling monitoring of the oxime reduction. As expected, the rate of reduction increased correspondingly, and resulted in complete reduction in less than 20 h (Figure 7b).

https://dx.doi.org/10.1021/acs.biomac.0c00620
Biomacromolecules 2020, 21, 2884–2895

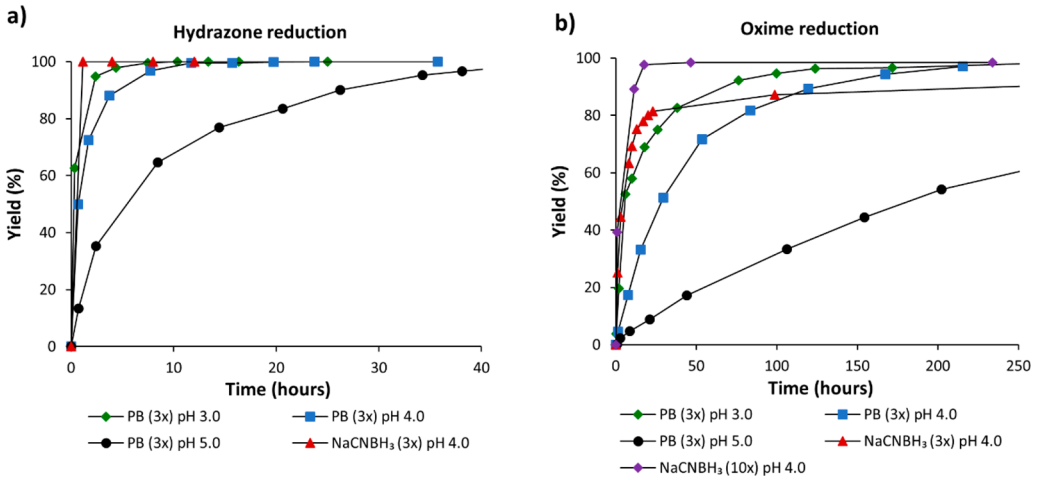

Figure 7. Reaction kinetics for the reduction of (a) A_nM-ADH conjugates (hydrazone reduction) and (b) A_nM-PDHA conjugates (oxime reduction) at pH 3.0, 4.0, and 5.0 using 3 equiv (3×) PB at RT. Reduction of conjugates at pH 4.0 using 3 or 10 equiv $NaCNBH_3$ at RT, is included in the figures for comparison.

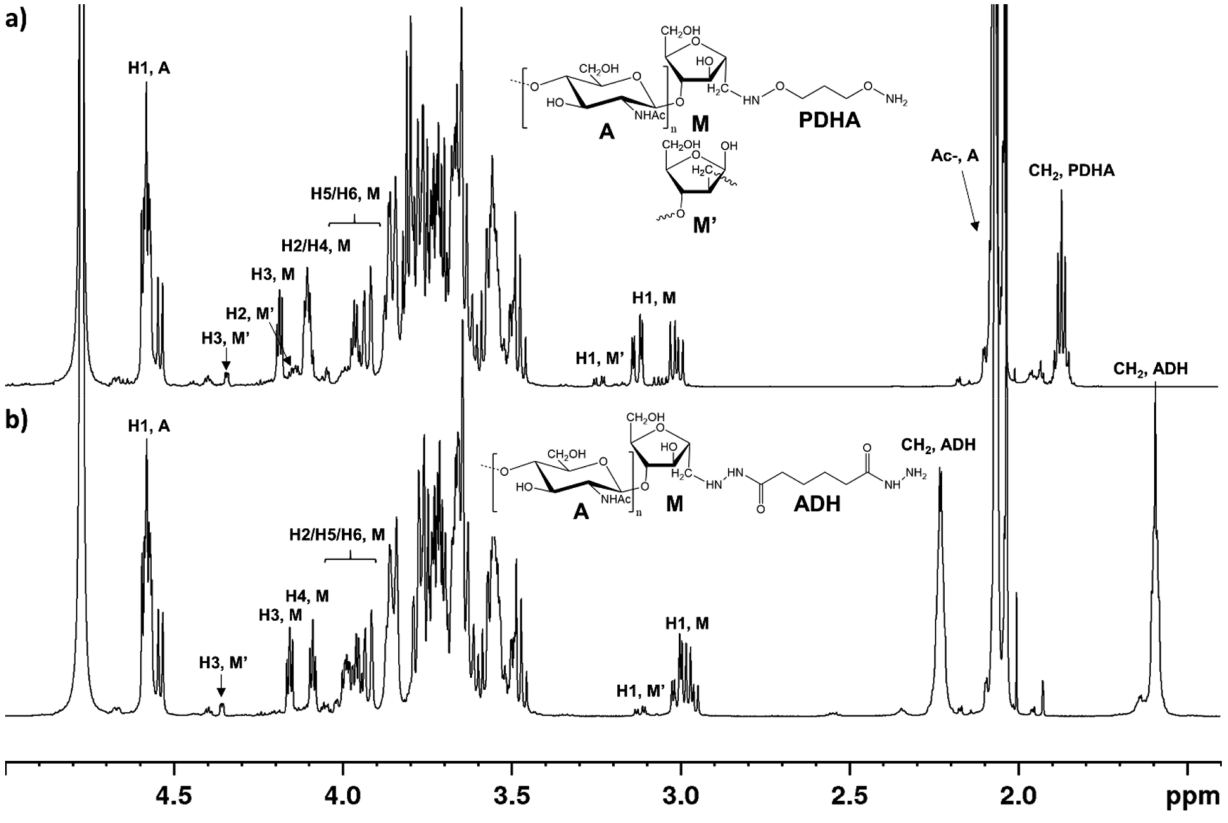

Figure 8. ^1H NMR spectra of reduced and purified (a) A_5M-PDHA and (b) A_5M-ADH conjugates.

The kinetic data in Figure 7 could be fitted to the model for the reductive amination using the previously obtained rate constants for the formation and dissociation of hydrazones or oximes (Table 1), as well as the rate constants for aldehyde reduction (Table 2). Hence, the rate of hydrazone or oxime reduction (assumed being irreversible and *E*- and *Z*-forms being equally reactive) became the only adjustable kinetic parameter. In general, reasonably good fits were obtained (Supporting Information, S8). The obtained rate constants for the reductions are given in Table 2. Interestingly, somewhat better fits were obtained by lowering the rate constants for A_nM reduction compared to reactions with A_nM and PB alone. The reason for this is presently not clear.

Preparative Protocols for Reduced A_nM-ADH/PDHA Conjugates. The results above provide the necessary information to develop protocols for preparative work. The most important is to maximize the conversion, but also to minimize the formation of disubstituted ADH or PDHA, for example, A_nM-ADH-MA_n,[5] as they are not reactive toward a second block. Assuming equal reactivity of both ends of ADH or PDHA, the statistical fraction of disubstituted species (f_{DS}), is given by the expression

https://dx.doi.org/10.1021/acs.biomac.0c00620
Biomacromolecules 2020, 21, 2884−2895

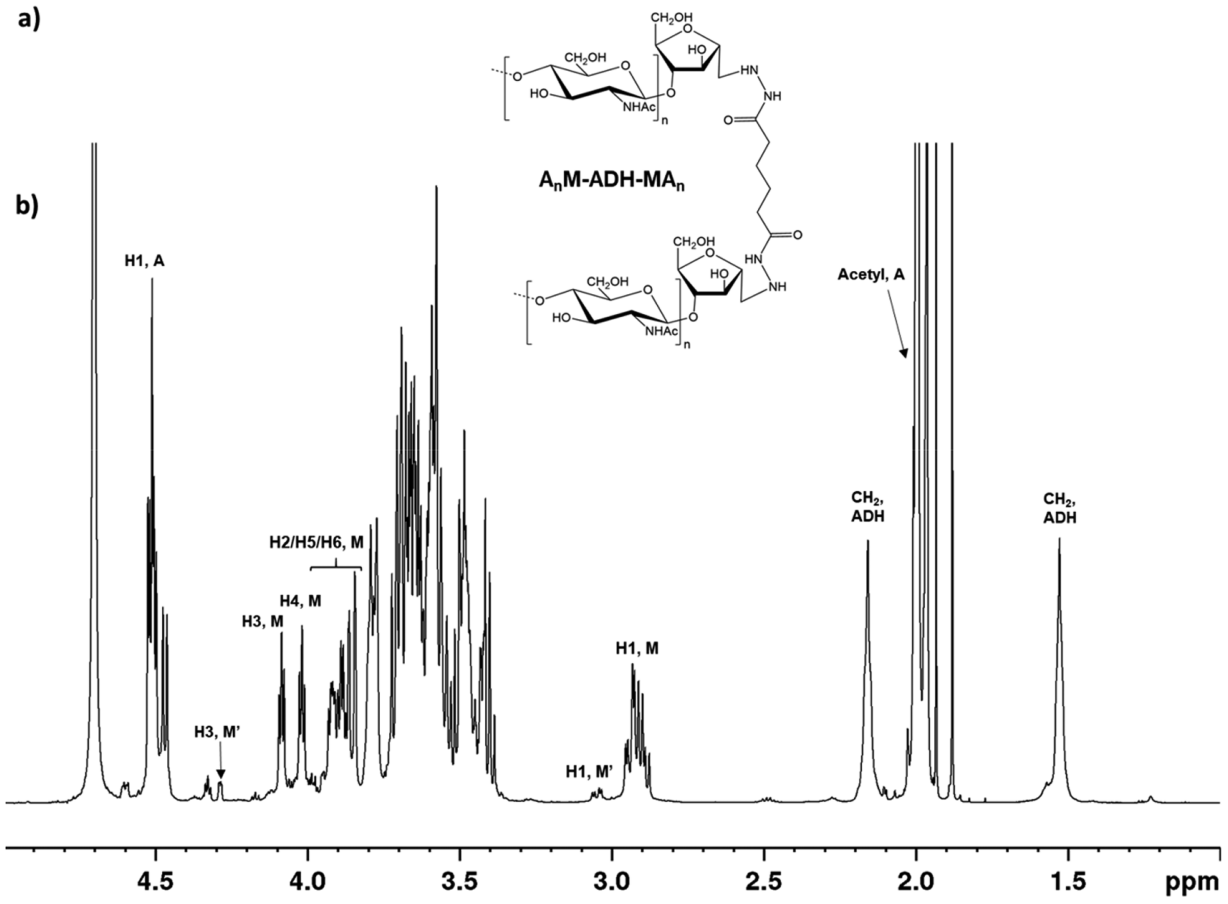

Figure 9. (a) General structure of the A_nM-ADH-MA_n diblock. (b) ^{1}H NMR spectrum of the reduced and purified A_4M-ADH-MA_4 diblock.

$$f_{DS} = \left(\frac{b}{2a}\right)^2$$

where b is the molar fraction of substituted oligosaccharide (from yield in Table 1), and a is the equivalence of a linker (PDHA or ADH). Derivation of the equation and examples are given in Supporting Information (S9). For example, 2 equiv (40.2 mM) ADH and a b of 0.87 (from Table 1, at pH 4.0) give 5% disubstituted ADH, which reduces to 0.2% with 10 equiv (201 mM). Hence, a large excess of ADH or PDHA is recommended, even when 2 equiv give acceptable conjugation yields. Although possibly interesting in other contexts, disubstituted species prevent further attachment of a second (different) block. The observation that the second attachment may be faster than the first further emphasizes the need for a high concentration of ADH or PDHA.

Because of the rapid reduction of unreacted A_nM oligomers, the reducing agent should be added after 4−6 h of conjugation. As shown above, 3 equiv of PB and a reduction time of 24 h (RT) is sufficient for quantitative reduction of A_nM-ADH conjugates. To overcome the slower reduction of oximes, 20 equiv of PB and a reaction time of 48 h is needed to give complete reduction of A_nM-PDHA conjugates (Supporting Information, S9). Alternatively, 10 equiv of $NaCNBH_3$ and a reaction time of 20 h is sufficient for quantitative reduction of PDHA conjugates, whereas 3 equiv and less than 1 h gives complete reduction of ADH conjugates. A_5M-ADH and A_5M-PDHA conjugates were prepared by the above-mentioned preparative protocols using PB as the reductant (Supporting Information, S9). ^{1}H NMR spectra of purified (GFC) and fully reduced A_5M-ADH and A_5M-PDHA conjugates are given in Figure 8. Annotations in the spectra are based on literature data[19] and the NMR characterization of purified and fully reduced A_2M-PDHA (Supporting Information, S10), where one of the alternative forms of the M residue was structurally elucidated (showed and annotated in Figure 8 as M′). In contrast to the main M residue, M′ can appear in equilibrium with the open ring, with two aldehydes at the reducing end. However, conjugates corresponding to the open form were not identified, and hence, it appears that the oligomers with the alternative form of the M residue react with both ADH and PDHA in the same way as oligomers with the main form (with the possible exception of a bit slower kinetics discussed above). The different forms cannot be separated during purification and without further investigation, we assume that the alternative forms cannot be distinguished when part of a diblock polysaccharide.

Attaching a Second Block: A_nM-*b*-MA_n Diblock Oligosaccharides. An efficient protocol to prepare A_nM-ADH/PDHA conjugates paves the way for attaching a second oligosaccharide in order to prepare chitin-based diblock oligo- or polysaccharides (A_nM-*b*-X). We first investigated the formation of A_nM-ADH-MA_n diblocks (Figure 9a). To study this, reduced A_4M-ADH conjugates were prepared and subsequently reacted with an equimolar amount of A_4M (conditions otherwise as above). The choice of equimolar proportions is based on the general need to use minimum amounts of oligosaccharide and also to simplify the following purification step. The amination was studied by time-course NMR as above, and rate constants are included in Table 1. The

https://dx.doi.org/10.1021/acs.biomac.0c00620
Biomacromolecules 2020, 21, 2884−2895

Table 3. Kinetic Parameters Obtained from the Modeling of the Conjugation of A ($Dext_m$) to B (ADH, PDHA or A_5M-ADH or A_5M-PDHA) Using Different Equivalents of B[a]

		A + B ↔ E		A + B ↔ Z		E ↔ Pyr		Z ↔ Pyr		
A	B (2×)	k_1 (h^{-1})	k_{-1} (h^{-1})	k_2 (h^{-1})	k_{-2} (h^{-1})	k_3 (h^{-1})	k_{-3} (h^{-1})	k_4 (h^{-1})	k_{-4} (h^{-1})	equilibrium yield (%)
$Dext_5$	ADH	1.5×10^{-3}	1.0×10^{1}	1.5×10^{-4}	1.0×10^{1}	1.1×10^{2}	1.1×10^{0}	1.1×10^{2}	1.1×10^{0}	35
$Dext_5$	PDHA	2.9×10^{-3}	2.0×10^{-3}	4.0×10^{-4}	1.5×10^{-1}	2.0×10^{0}	6.8×10^{0}	2.7×10^{1}	2.0×10^{1}	87
A	B (1×)									
$Dext_6$	A_5M-ADH	3.0×10^{-3}	1.7×10^{1}	3.0×10^{-4}	1.7×10^{1}	1.1×10^{2}	1.1×10^{0}	1.1×10^{2}	1.1×10^{0}	15
$Dext_6$	A_5M-PDHA	1.1×10^{-2}	5.0×10^{-2}	1.5×10^{-3}	1.0×10^{-1}	1.9×10^{0}	4.5×10^{0}	2.7×10^{1}	1.5×10^{1}	66

[a]Reactions were performed at pH 4.0, RT. E: *E*-hydrazone/oxime. Z: *Z*-hydrazone/oxime. Pyr: *N*-pyranoside.

total equilibrium yield of hydrazones was as high as 74% with only one equivalent of the second block. To allow a more direct comparison, we used the rate constants for the conjugation of A_2M and A_5M to free ADH (2 equiv) to simulate the rate ($t_{0.5}$ and $t_{0.9}$) and yield for the reaction with equimolar proportions of oligomers and amines (Supporting Information, S11). Interestingly, the equilibrium yield was lower, and the rate was lower than for the conjugation of A_4M to the A_4M-ADH conjugate, indicating that the reactivity of the free hydrazide group toward terminal M-residues is higher for A_nM-ADH than for free ADH (Supporting Information, S11). After subsequent reduction with PB (3 equiv) the relative yield of A_nM-ADH-MA_n diblocks was approximately 83% (obtained by integration of the GFC chromatogram, Supporting Information, S11). Unreacted A_4M oligomers were completely reduced, hence, preventing the diblock formation from going to completion. The general structure of the A_nM-ADH-MA_n diblocks and ^{1}H NMR spectrum of the reduced and purified A_4M-ADH-MA_4 diblock are given in Figure 9.

The diblock formation was further investigated in the special case of 0.5 equiv of ADH or PDHA to A_2M oligomers. These conditions should at completion give only disubstituted ADH/PDHA, that is, the diblocks A_2M-ADH-MA_2 and A_2M-PDHA-MA_2. Here, faster conjugation was observed, especially for ADH, supporting the theory of different kinetics for the attachment of the second block (Table 1 and Supporting Information, S12). High equilibrium yields of hydrazones and oximes were obtained (73% with ADH and 86% with PDHA). Interesting, the yield of diblocks after reduction was not increased above these values (Supporting Information, S12). Hence, the yield of diblocks corroborates with the statistical amount of disubstituted species expected for the systems (as equimolar concentration of amine and oligomer was used).

Attaching a Second Block: A_nM-*b*-Dextran Diblock Oligosaccharides. The final step was to study the attachment of a second block of a different kind, namely dextran, using purified and reduced A_5M-ADH and A_5M-PDHA conjugates to form chitin-*b*-dextran diblocks. Dextran oligomers ($Dext_m$) of defined DP (m = DP) were obtained by partial hydrolysis of dextran and fractionation of oligomers by gel filtration chromatography (Supporting Information, S13). Reactions were monitored by time course NMR, again using equimolar amounts of the two blocks.

By this strategy the reactivity of the reducing end of $Dext_m$ governs the conjugation. Therefore, the kinetics of the conjugation of $Dext_5$ to free ADH and PDHA (2 equiv) was included for comparison (Supporting Information, S14). Importantly, dextran forms *N*-pyranosides in addition to *E*- and *Z*-oximes with PDHA, whereas it forms almost exclusively *N*-pyranosides with ADH.[5,32] Kinetic constants are given in Table 3.

It may first be noted that dextran oligomers, in agreement with previous findings,[5] are much less reactive toward ADH and PDHA compared to A_nM oligomers (data for A_nM in Table 1). This is due to the pending aldehyde of the reducing end of the latter being more reactive, as it does not participate in an aldehyde/hemiacetal equilibrium. Second, the rate constants for forming *N*-pyranosides (k_3 and k_4) are 2 orders of magnitude larger for ADH compared to PDHA. For ADH, they are 5−6 orders of magnitude larger than k_1 and k_2. Hence, the first step (*E*- and *Z*-formation) is rate limiting, although *E*- and *Z*-hydrazones are hardly detected during the reaction with ADH.

The rate constants in Table 3 suggest that dextran oligomers react faster with A_nM-ADH and A_nM-PDHA compared to free ADH and PDHA. To allow a more direct comparison, we used the rate constants for the conjugation of $Dext_5$ to free ADH (2 equiv) to simulate the rate ($t_{0.5}$ and $t_{0.9}$) and yield for the reaction with equimolar proportions of $Dext_5$ and amines (Supporting Information, S15). As observed for the A_nM oligomers, dextran reacted faster, and resulted in a higher yield, with the A_5M-ADH or -PDHA conjugates than with free ADH or PDHA. Hence, the second attachment is indeed faster in both cases.

Equilibrium yields obtained with equimolar amounts of dextran and A_5M-ADH/PDHA were only 15% for ADH, but 66% for PDHA. However, improved yields can be expected during reduction of the equilibrium mixture because of the slow reduction of unreacted dextran. Since dextran-based hydrazones and oximes are slowly reduced by PB at RT,[5] the reduction was performed using 20 equiv PB at increased temperature (40 °C). Reaction products were fractionated by GFC and analyzed by ^{1}H NMR (Supporting Information, S15).

By integration of the GFC chromatogram, the relative yield of A_5M-PDHA-$Dext_6$ diblocks was 92% after 72 h, whereas for A_5M-ADH-$Dext_6$, we obtained about 85% diblocks after 144 h of reduction (Supporting Information, S15). The higher yield and shorter reaction times for PDHA diblocks is partly ascribed to the higher equilibrium yield prior to reduction. Moreover, the almost complete formation of *N*-pyranosides reduces the reduction rate of dextran-ADH conjugates considerably.[5] It may also be noted that at 40 °C some reduction of unreacted dextran occurred (Supporting Information, S15), but the rate was low compared to reduction of unreacted A_nM. Hence, an increased yield of diblocks can be obtained after addition of reductant in the dextran systems compared to the A_nM systems. The general structures of chitin-*b*-dextran diblocks prepared with ADH and PDHA and

https://dx.doi.org/10.1021/acs.biomac.0c00620
Biomacromolecules 2020, 21, 2884−2895

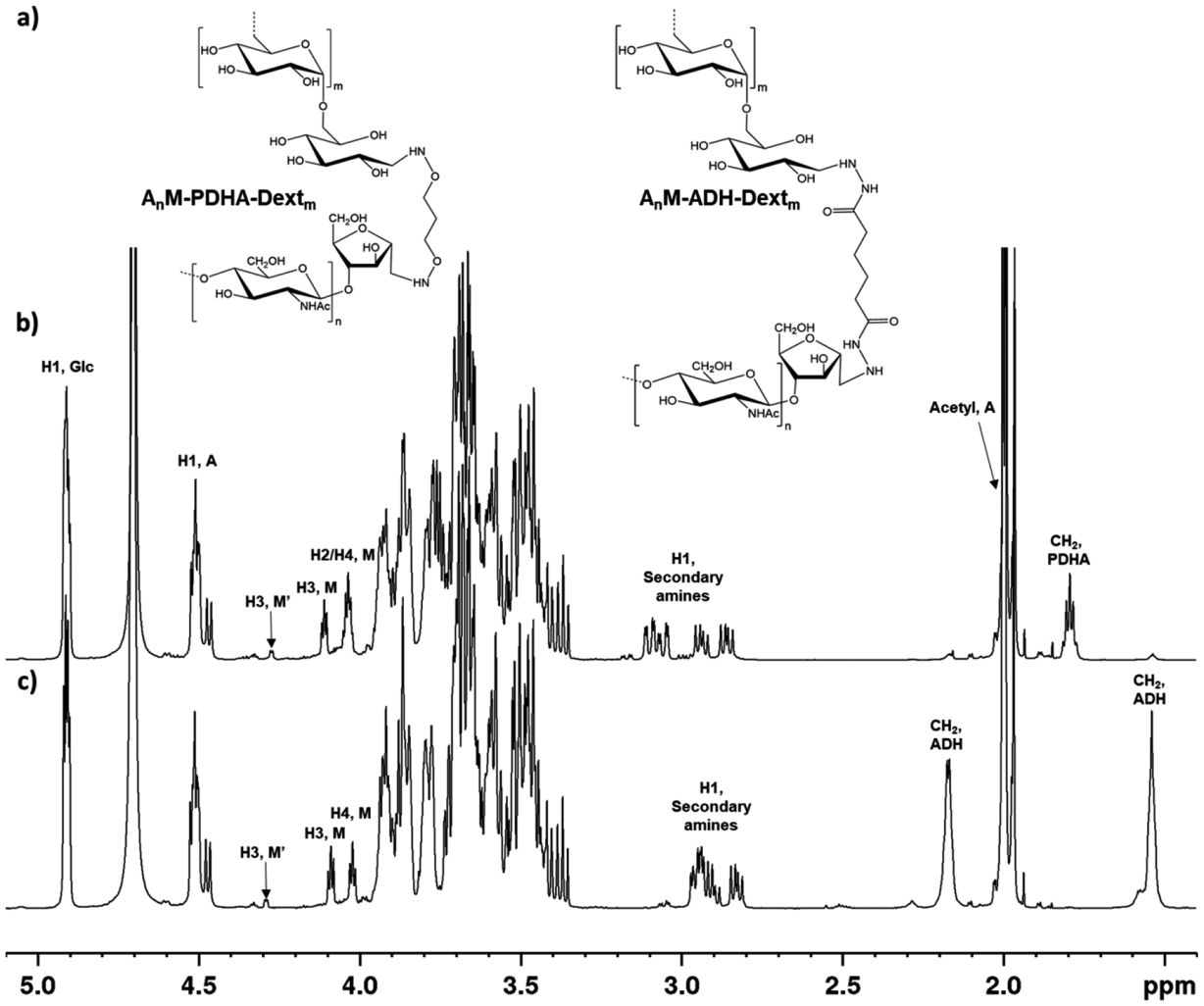

Figure 10. (a) General structure of chitin-*b*-dextran diblocks prepared with ADH or PDHA. ^{1}H NMR spectra of the reduced and purified (b) A_5M-PDHA-Dext$_6$ diblock and the (c) A_5M-ADH-Dext$_6$ diblock.

^{1}H NMR spectra of reduced and purified A_5M-*b*-Dext$_6$ diblocks are given in Figure 10.

Based on the results of this study, two strategies for the preparation of A_nM-*b*-dextran block polysaccharides can be proposed. For the strategy where dextran is conjugated to the free end of ADH or PDHA in A_nM conjugates (discussed above), the attachment of the second block is time-consuming since dextran oligomers react more slowly with ADH/PDHA compared to the highly reactive A_nM oligomers. Moreover, the reduction of dextran-based hydrazones and oximes also is slow. However, in contrast to the A_nM oligomers, unreacted dextran oligomers are reduced at a low rate under the given conditions and hence, a high yield of diblocks can be obtained (even under equimolar proportions), even though this strategy requires long reaction times for attachment of the second block.

An alternative strategy is to reverse the protocol and prepare ADH- or PDHA-activated dextran oligomers in the first step. Due to the slow reduction of dextran oligomers, activation using a large excess of ADH or PDHA can be performed as a conventional one-pot reductive amination. The subsequent conjugation of A_nM oligomers to the free end of ADH or PDHA takes advantage of the high reactivity of the terminal M residue of the A_nM oligomers, and the attachment of the second block (both conjugation and reduction) is time-efficient compared to opposite strategy. However, this strategy is restricted by the rapid reduction of unreacted A_nM oligomers, which will limit the yield of diblocks (if reacted in an equimolar ratio).

An excess of one of the blocks will in both strategies lead to faster kinetics and a higher yield of diblocks. However, an excess of the second block will render some or all the unreacted oligomers inactive after reduction (most relevant for an excess of A_nM oligomers, but also relevant for dextran oligomers, as shown above). An excess of the activated oligomer conjugate will in contrast be beneficial in both strategies as activated oligomers can be recycled. Both the above-mentioned strategies require purification after diblock formation, and in this study, GFC was proven useful. However, purification by block-specific solvents is clearly a possibility deserving future attention. Hence, which strategy is better therefore depends on factors such as which oligomer or conjugate can be used in excess ("value" of reactants) and the available purification steps. It may also be noted that improved equilibrium yields can be obtained by increasing the absolute concentrations of reactants. However, higher concentrations are not compatible with very long chains due to solubility and viscosity issues, and in any case, the reductant (PB) will

https://dx.doi.org/10.1021/acs.biomac.0c00620
Biomacromolecules 2020, 21, 2884−2895

certainly be insoluble at very high concentrations. Heterogeneous systems may be worth exploring further, but this is outside the scope of the present work.

The strategies described above should also be relevant for chitosan oligomers prepared by nitrous acid degradation (D_nM type). However, self-branching is an issue for such oligomers.[18] Hence, the strategy where an excess of activated conjugates is used will be advantageous for such oligomers.

CONCLUSIONS

In this work we have first studied in detail the activation of chitin oligosaccharides with the highly reactive 2,5-anhydro-D-mannose at the reducing end (A_nM) by ADH and PDHA as a basis for the preparation of chitin-based diblock polysaccharides. Kinetic constants for both the formation and dissociation of oximes and hydrazones, as well as for their irreversible reduction to the corresponding secondary amines using PB were determined. Rate constants were essentially independent of the chain length and could be used to model the reactions for a wide range of concentrations of reagents. The high susceptibility to reduction of M residues (by both PB and $NaCNBH_3$) was circumvented by a two-step procedure thanks to the excellent equilibrium yields prior to reduction. The free ends of ADH or PDHA activated oligomers had higher reactivities compared to free ADH or PDHA. Hence, attachment of a second block to form diblocks was therefore feasible and could easily be modeled kinetically. Examples include A_nM-*b*-MA_n and A_nM-*b*-dextran. For the latter, a "reverse" strategy of reacting A_nM with ADH- or PDHA-activated dextran is also a viable alternative thanks to the high reactivity of the terminal M residue.

Regarding potential applications, water-soluble chitin oligomers activated with PDHA or ADH would be ideally suited for conjugation with biomolecules in aqueous solvents. Strong phase separation of copolymers containing chitin blocks is also expected in solution or in the bulk due to the very high solubility parameter of chitin.[33,34] A wide range of self-assembled structures could then potentially be obtained from chitin-based block copolymers. Chitin, including chitin oligomers, is also known to play important roles in activating immune responses against fungal pathogens in both mammals[35] and in plants[36] and are used in the agricultural industry as plant growth stimulators.[37] Terminally conjugated chitin-based block polymers or block polysaccharides hence offer a wide range of new and possibly bioactive materials. These may, on one hand, take advantage of the uninterrupted chitin sequences needed for interacting with chitin receptors and, on the other hand, have additional bioactivities due to the second chain.

ASSOCIATED CONTENT

Supporting Information

The Supporting Information is available free of charge at https://pubs.acs.org/doi/10.1021/acs.biomac.0c00620.

Additional data and explanations are given in S1− S15 (PDF)

AUTHOR INFORMATION

Corresponding Authors

Christophe Schatz − *Laboratoire de Chimie des Polymères Organiques (LCPO), Université de Bordeaux, 33600 Pessac, France*; Email: schatz@enscbp.fr

Bjørn E. Christensen − *NOBIPOL, Department of Biotechnology and Food Science, NTNU - Norwegian University of Science and Technology, Trondheim, Norway*; orcid.org/0000-0001-9640-0225; Email: bjorn.e.christensen@ntnu.no

Authors

Ingrid Vikøren Mo − *NOBIPOL, Department of Biotechnology and Food Science, NTNU - Norwegian University of Science and Technology, Trondheim, Norway*

Marianne Øksnes Dalheim − *NOBIPOL, Department of Biotechnology and Food Science, NTNU - Norwegian University of Science and Technology, Trondheim, Norway*

Finn L. Aachmann − *NOBIPOL, Department of Biotechnology and Food Science, NTNU - Norwegian University of Science and Technology, Trondheim, Norway*; orcid.org/0000-0003-1613-4663

Complete contact information is available at: https://pubs.acs.org/10.1021/acs.biomac.0c00620

Notes

The authors declare no competing financial interest.

ACKNOWLEDGMENTS

This work was supported by a grant from the Norwegian University of Science and Technology to I.V. Mo, and Grants 268490, 226244, and 221576 from the Research Council of Norway. C.S. wishes to thank the Agence Nationale de la Recherche for its support under the program TANGO (ANR-16-CE09-0020-01).

REFERENCES

(1) Volokhova, A. S.; Edgar, K. J.; Matson, J. B. Polysaccharide-containing block copolymers: synthesis and applications. *Mater. Chem. Front.* **2020**, *4*, 99−112.

(2) Schatz, C.; Lecommandoux, S. Polysaccharide-Containing Block Copolymers: Synthesis, Properties and Applications of an Emerging Family of Glycoconjugates. *Macromol. Rapid Commun.* **2010**, *31* (19), 1664−1684.

(3) Novoa-Carballal, R.; Muller, A. H. E. Synthesis of polysaccharide-b-PEG block copolymers by oxime click. *Chem. Commun.* **2012**, *48* (31), 3781−3783.

(4) Bondalapati, S.; Ruvinov, E.; Kryukov, O.; Cohen, S.; Brik, A. Rapid End-Group Modification of Polysaccharides for Biomaterial Applications in Regenerative Medicine. *Macromol. Rapid Commun.* **2014**, *35* (20), 1754−1762.

(5) Mo, I. V.; Feng, Y.; Dalheim, M. Ø.; Solberg, A.; Aachmann, F. L.; Schatz, C.; Christensen, B. E. Activation of enzymatically produced chitooligosaccharides by dioxyamines and dihydrazides. *Carbohydr. Polym.* **2020**, *232*, 115748.

(6) Xiao, Y.; Chinoy, Z. S.; Pecastaings, G.; Bathany, K.; Garanger, E.; Lecommandoux, S. Design of Polysaccharide-b-Elastin-Like Polypeptide Bioconjugates and Their Thermoresponsive Self-Assembly. *Biomacromolecules* **2020**, *21* (1), 114−125.

(7) Rosselgong, J.; Chemin, M.; Almada, C. C.; Hemery, G.; Guigner, J.-M.; Chollet, G.; Labat, G.; Da Silva Perez, D.; Ham-Pichavant, F.; Grau, E.; Grelier, S.; Lecommandoux, S.; Cramail, H. Synthesis and Self-Assembly of Xylan-Based Amphiphiles: From Bio-Based Vesicles to Antifungal Properties. *Biomacromolecules* **2019**, *20* (1), 118−129.

(8) Tiwari, V. K.; Mishra, B. B.; Mishra, K. B.; Mishra, N.; Singh, A. S.; Chen, X. Cu-Catalyzed Click Reaction in Carbohydrate Chemistry. *Chem. Rev.* **2016**, *116* (5), 3086−3240.

(9) Breitenbach, B. B.; Schmid, I.; Wich, P. R. Amphiphilic Polysaccharide Block Copolymers for pH-Responsive Micellar Nanoparticles. *Biomacromolecules* **2017**, *18* (11), 3844−3845.

(10) Feng, F.; Sun, J.; Radhakrishnan, G. V.; Lee, T.; Bozsoki, Z.; Fort, S.; Gavrin, A.; Gysel, K.; Thygesen, M. B.; Andersen, K. R.; Radutoiu, S.; Stougaard, J.; Oldroyd, G. E. D. A combination of chitooligosaccharide and lipochitooligosaccharide recognition promotes arbuscular mycorrhizal associations in Medicago truncatula. *Nat. Commun.* **2019**, *10* (1), 5047.
(11) Ahmed, A. B. A.; Taha, R. M.; Mohajer, S.; Elaagib, M. E.; Kim, S. K. Preparation, properties and biological applications of water soluble chitin oligosaccharides from marine organisms. *Russ. J. Mar. Biol.* **2012**, *38* (4), 351−358.
(12) Roby, D.; Gadelle, A.; Toppan, A. Chitin oligosaccharides as elicitors of Chitinase activity in melon plants. *Biochem. Biophys. Res. Commun.* **1987**, *143* (3), 885−892.
(13) Azuma, K.; Osaki, T.; Minami, S.; Okamoto, Y. Anticancer and Anti-Inflammatory Properties of Chitin and Chitosan Oligosaccharides. *J. Funct. Biomater.* **2015**, *6* (1), 33−49.
(14) Kadokawa, J.-I.; Karasu, M.; Tagaya, H.; Chiba, K. Synthesis of a Block Copolymer Consisting of Oligocellulose and Oligochitin. *J. Macromol. Sci., Part A: Pure Appl.Chem.* **1996**, *33* (11), 1735−1743.
(15) Kadokawa, U.-I.; Yamashita, K.; Karasu, M.; Tagaya, H.; Chiba, K. Preparation and Enzymatic Hydrolysis of Block Copolymer Consisting of Oligochitin and Poly(Propylene Glycol). *J. Macromol. Sci., Part A: Pure Appl.Chem.* **1995**, *32* (7), 1273−1280.
(16) Allan, G. G.; Peyron, M. Molecular-Weight Manipulation of Chitosan 0.1. Kinetics of Depolymerization by Nitrous-Acid. *Carbohydr. Res.* **1995**, *277* (2), 257−272.
(17) Tømmeraas, K.; Vårum, K. M.; Christensen, B. E.; Smidsrød, O. Preparation and characterisation of oligosaccharides produced by nitrous acid depolymerisation of chitosans. *Carbohydr. Res.* **2001**, *333* (2), 137−144.
(18) Tømmeraas, K.; Strand, S. P.; Christensen, B. E.; Smidsrød, O.; Vårum, K. M. Preparation and characterization of branched chitosans. *Carbohydr. Polym.* **2011**, *83* (4), 1558−1564.
(19) Moussa, A.; Crepet, A.; Ladaviere, C.; Trombotto, S. Reducing-end ″clickable″ functionalizations of chitosan oligomers for the synthesis of chitosan-based diblock copolymers. *Carbohydr. Polym.* **2019**, *219*, 387−394.
(20) Pickenhahn, V. D.; Darras, V.; Dziopa, F.; Biniecki, K.; De Crescenzo, G.; Lavertu, M.; Buschmann, M. D. Regioselective thioacetylation of chitosan end-groups for nanoparticle gene delivery systems. *Chem. Sci.* **2015**, *6* (8), 4650−4664.
(21) Coudurier, M.; Faivre, J.; Crepet, A.; Ladaviere, C.; Delair, T.; Schatz, C.; Trombotto, S. Reducing-End Functionalization of 2,5-Anhydro-d-mannofuranose-Linked Chitooligosaccharides by Dioxyamine: Synthesis and Characterization. *Molecules* **2020**, *25* (5), 1143.
(22) Ruhaak, L. R.; Steenvoorden, E.; Koeleman, C. A. M.; Deelder, A. M.; Wuhrer, M. 2-Picoline-borane: A non-toxic reducing agent for oligosaccharide labeling by reductive amination. *Proteomics* **2010**, *10* (12), 2330−2336.
(23) Cosenza, V. A.; Navarro, D. A.; Stortz, C. A. Usage of α-picoline borane for the reductive amination of carbohydrates. *ARKIVOC* **2011**, *12*, 182−194.
(24) Fang, J.; Qin, G.; Ma, J.; She, Y.-M. Quantification of plant cell wall monosaccharides by reversed-phase liquid chromatography with 2-aminobenzamide pre-column derivatization and a non-toxic reducing reagent 2-picoline borane. *J. Chromatogr. A* **2015**, *1414*, 122−128.
(25) Unterieser, I.; Mischnick, P. Labeling of oligosaccharides for quantitative mass spectrometry. *Carbohydr. Res.* **2011**, *346* (1), 68−75.
(26) Chen, J.; Spiering, G.; Mosquera-Giraldo, L.; Moore, R. B.; Edgar, K. J. Regioselective Bromination of the Dextran Nonreducing End Creates a Pathway to Dextran-Based Block Copolymers. *Biomacromolecules* **2020**, *21*, 1729−1738.
(27) Li, B.; Wang, Q.; Wang, X.; Wang, C.; Jiang, X. Preparation, drug release and cellular uptake of doxorubicin-loaded dextran-*b*-poly(ε-caprolactone) nanoparticles. *Carbohydr. Polym.* **2013**, *93* (2), 430−437.
(28) Vårum, K. M.; Antohonsen, M. W.; Grasdalen, H.; Smidsrød, O. Determination of the degree of N-acetylation and the distribution of N-acetyl groups in partially N-deacetylated chitins (chitosans) by high-field n.m.r. spectroscopy. *Carbohydr. Res.* **1991**, *211* (1), 17−23.
(29) Lindberg, B.; Lönngren, J.; Svensson, S., Specific Degradation of Polysaccharides. In *Adv. Carbohydr. Chem. Biochem.*; Tipson, R. S., Derek, H., Eds.; Academic Press, 1975; Vol. *31*, pp 185−240.
(30) Baudendistel, O. R.; Wieland, D. E.; Schmidt, M. S.; Wittmann, V. Real-Time NMR Studies of Oxyamine Ligations of Reducing Carbohydrates under Equilibrium Conditions. *Chem. - Eur. J.* **2016**, *22* (48), 17359−17365.
(31) Gilmore, K.; Vukelić, S.; McQuade, D. T.; Koksch, B.; Seeberger, P. H. Continuous Reductions and Reductive Aminations Using Solid NaBH4. *Org. Process Res. Dev.* **2014**, *18* (12), 1771−1776.
(32) Kwase, Y. A.; Cochran, M.; Nitz, M., Protecting-Group-Free Glycoconjugate Synthesis: Hydrazide and Oxyamine Derivatives in N-Glycoside Formation. In *Modern Synthetic Methods in Carbohydrate Chemistry: From Monosaccharides to Complex Glycoconjugates*; Werz, D. B., Vidal, S., Eds.; Wiley, 2013; pp 67−96.
(33) Ravindra, R.; Krovvidi, K. R.; Khan, A. A. Solubility parameter of chitin and chitosan. *Carbohydr. Polym.* **1998**, *36* (2), 121−127.
(34) Lehnert, R. J.; Kandelbauer, A. Comments on "Solubility parameter of chitin and chitosan" Carbohydrate Polymers 36 (1998) 121−127. *Carbohydr. Polym.* **2017**, *175*, 601−602.
(35) Fuchs, K.; Cardona Gloria, Y.; Wolz, O.-O.; Herster, F.; Sharma, L.; Dillen, C. A.; Täumer, C.; Dickhöfer, S.; Bittner, Z.; Dang, T.-M.; Singh, A.; Haischer, D.; Schlöffel, M. A.; Koymans, K. J.; Sanmuganantham, T.; Krach, M.; Roger, T.; Le Roy, D.; Schilling, N. A.; Frauhammer, F.; Miller, L. S.; Nürnberger, T.; LeibundGut-Landmann, S.; Gust, A. A.; Macek, B.; Frank, M.; Gouttefangeas, C.; Dela Cruz, C. S.; Hartl, D.; Weber, A. N. The fungal ligand chitin directly binds TLR2 and triggers inflammation dependent on oligomer size. *EMBO Rep.* **2018**, *19* (12), e46065.
(36) Gao, F.; Zhang, B.-S.; Zhao, J.-H.; Huang, J.-F.; Jia, P.-S.; Wang, S.; Zhang, J.; Zhou, J.-M.; Guo, H.-S. Deacetylation of chitin oligomers increases virulence in soil-borne fungal pathogens. *Nature Plants* **2019**, *5* (11), 1167.
(37) Schmitz, C.; González Auza, L.; Koberidze, D.; Rasche, S.; Fischer, R.; Bortesi, L. Conversion of Chitin to Defined Chitosan Oligomers: Current Status and Future Prospects. *Mar. Drugs* **2019**, *17* (8), 452.

https://dx.doi.org/10.1021/acs.biomac.0c00620
Biomacromolecules 2020, 21, 2884−2895